SIAM J. NUMER. ANAL.
Vol. 31, No. 5, pp. 1497-1518, October 1994

012

COMPUTATION OF THE COMPLEX ERROR FUNCTION*

J. A. C. WEIDEMAN†

Abstract. Rational expansions for computing the complex error function $w(z) = e^{-z^2}\operatorname{erfc}(-iz)$ are presented. These expansions have the following attractive properties: (1) they can be evaluated using a polynomial evaluation routine such as Horner's method, (2) the polynomial coefficients can be computed once and for all by a single Fast Fourier Transform (FFT), and (3) high accuracy is achieved uniformly in the complex plane with only a small number of terms. Comparisons reveal that in some parts of the complex plane certain competitors may be more efficient. However, the difference in efficiency is never great, and the new algorithms are simpler than existing ones: a complete program takes eight lines of Matlab code.

Key words. complex error function, orthogonal rational expansions, steepest descent, Fast Fourier Transform

AMS subject classifications. 65D20, 33B20

1. Introduction.

The complex error function and its complement

$$\operatorname{erf}(z) = \frac{2}{\sqrt{\pi}} \int_0^z e^{-t^2}\, dt, \qquad \operatorname{erfc}(z) = \frac{2}{\sqrt{\pi}} \int_z^\infty e^{-t^2}\, dt = 1 - \operatorname{erf}(z), \tag{1}$$

as well as Dawson's integral

$$\operatorname{daw}(z) = e^{-z^2} \int_0^z e^{t^2}\, dt, \qquad z \in \mathbb{C}, \tag{2}$$

arise in many branches of science. Equally abundant are methods for evaluating these functions. These range from tables [10], [11], [28] to modern software [13], [17], [24], [27], [30], some of which will be discussed below.

In this paper we aspire to make yet another contribution to this well-trodden field. We present rational approximations with primarily two attractive properties: First, they provide high accuracy *uniformly* in the complex plane with certain regions where exceptional accuracy is achieved. Second, the ease of coding of our method can hardly be surpassed. All it requires is a polynomial evaluation routine such as the Horner algorithm. One Fast Fourier Transform (FFT) of modest length computes the coefficients, and this needs to be done only once. To anticipate ourselves, the eight line Matlab program in Table 1 does it all.

Perhaps the most fundamental member in this family is the Faddeeva function, also referred to as the plasma dispersion function [10], [11]

$$w(z) = e^{-z^2}\operatorname{erfc}(-iz).$$

Many algorithms, including our own, focus on this function and then obtain the values of (1)–(2) by elementary relations (see [14], [26]).

* Received by the editors August 2, 1993; accepted for publication August 16, 1993. The work of this author was supported in part by the Advanced Computing Research Institute and the Center for Applied Mathematics, Cornell University, and from National Science Foundation grant DMS-9116110 to L. N. Trefethen.

† Department of Mathematics, Oregon State University, Corvallis, Oregon 97331-4605 (weideman@math.orst.edu).

Our method is based on the integral representation [9], [11], [12]

$$w(z) = \frac{i}{\pi}\int_{-\infty}^{\infty} \frac{e^{-t^2}}{z-t}\,dt, \qquad \mathrm{Im}(z) > 0. \tag{3}$$

When $z = x \in \mathbb{R}$, this representation should be modified to

$$w(x) = e^{-x^2} + \frac{i}{\pi}\,\mathrm{PV}\int_{-\infty}^{\infty} \frac{e^{-t^2}}{x-t}\,dt = e^{-x^2} + \frac{2i}{\sqrt{\pi}}\,\mathrm{daw}(x), \tag{4}$$

where the principal value integral defines the Hilbert transform of e^{-t^2}. The paper [32], in which e^{-t^2} served as a test example for computing the Hilbert transform, motivated the present research.

We start by assuming the existence of an expansion

$$[W(t)]^{-1}e^{-t^2} = \sum_{n=-\infty}^{\infty} a_n\phi_n(t), \qquad t \in \mathbb{R}, \tag{5}$$

where $\{\phi_n(t)\}$ is an orthogonal basis set in $L_2(\mathbb{R}; W(t))$ with appropriate weight function $W(t)$. Then

$$\frac{e^{-t^2}}{z-t} = \sum_{n=-\infty}^{\infty} a_n\left[W(t)\frac{\phi_n(t)}{z-t}\right], \tag{6}$$

and term-by-term integration yields

$$w(z) = \sum_{n=-\infty}^{\infty} a_n\psi_n(z), \qquad \mathrm{Im}(z) > 0, \tag{7}$$

where

$$\psi_n(z) = \frac{i}{\pi}\int_{-\infty}^{\infty} W(t)\frac{\phi_n(t)}{z-t}\,dt. \tag{8}$$

We shall introduce sets $\{\phi_n(t)\}$ that possess the properties required to turn (5)–(8) into a practical algorithm. In particular, we shall show that with these functions the following occurs:

- The convergence of the series (7) is rapid, provided a certain scaling parameter L is chosen optimally. (Only 16 terms are sufficient for a relative error of better than 10^{-6}, uniformly for all z in the upper half-plane. See Fig. 4.)
- The integrals (8) are easily evaluated.
- The series (7) becomes an ordinary polynomial of a transformed variable, and can therefore be evaluated with a simple algorithm such as the Horner rule.
- The expansion coefficients a_n can be computed rapidly and efficiently with the FFT.

The outline of the paper is as follows. In §2 we introduce the first basis set $\{\phi_n(t)\}$ to be used in (5)–(8). Recurrence formulas for the expansion coefficients a_n are derived in §3. Asymptotic estimates for the rate of decay in the expansion coefficients are given in §4, and we also derive an estimate for the optimal value of the parameter L alluded to above. In §5 a second basis set is introduced, and alternative expansions are discussed. Implementation aspects and in particular the computation of the expansion coefficients are addressed in §6, where we also present numerical comparisons of the various expansions. A survey of algorithms for error functions is given in §7, and we compare our method with some of these.

2. First expansion. The first basis set we shall use in (5)–(8) is defined by

$$\sigma_n(t) = \left(\frac{L+it}{L-it}\right)^n. \tag{9}$$

basis for Im(z)>0 and Im(z)<0

L is a real, positive parameter to be chosen for optimal accuracy. The set $\{\sigma_n(t)\}$ is complete and orthogonal in $L_2(\mathbb{R}; W(t))$ with weight function $W(t) = 1/(L^2+t^2)$. This follows from noting that expansions in terms of $\{\sigma_n(t)\}$ are nothing but Fourier series. Introducing the real variable θ through

$$e^{i\theta} = \frac{L+it}{L-it}, \quad \text{i.e.,} \quad t = L\tan\frac{1}{2}\theta, \tag{10}$$

we map $t \in [-\infty, \infty]$ to $\theta \in [-\pi, \pi]$. Then

$$f(t) = \sum_{n=-\infty}^{\infty} a_n\sigma_n(t) \Longrightarrow f(t) = \sum_{n=-\infty}^{\infty} a_n e^{in\theta}.$$

The orthogonality relation for Fourier series $\int_{-\pi}^{\pi} e^{in\theta}e^{-im\theta}\,d\theta = 2\pi\delta_{m,n}$ translates into

$$\int_{-\infty}^{\infty} W(t)\sigma_n(t)\overline{\sigma_m(t)}\,dt = \frac{L}{\pi}\delta_{mn},$$

where the overbar denotes the complex conjugate and δ_{mn} is the Kronecker delta. The expansion coefficients are therefore given by

$$a_n = \frac{L}{\pi}\int_{-\infty}^{\infty} \frac{f(t)}{L^2+t^2}\left(\frac{L-it}{L+it}\right)^n dt.$$

Note that for real-valued even functions $f(t)$ it follows that $a_n \in \mathbb{R}$ for all n, as well as $a_n = a_{-n}$.

As a side remark we note that $\{\sigma_n(t)\}$, as well as the alternative set $\{\rho_n(t)\}$ described in §5, may be used as basis for spectral methods for solving differential equations on the real line. Such applications are described in [2], [3], [31].

We shall primarily be concerned with $f(t) = (L^2+t^2)e^{-t^2}$, and

$$a_n = \frac{L}{\pi}\int_{-\infty}^{\infty} e^{-t^2}\left(\frac{L-it}{L+it}\right)^n dt. \tag{11}$$

To investigate the convergence of the series (5)–(7), we need to estimate a_n as $n \to \infty$. An asymptotic analysis is postponed to §4. For the present we simply integrate (11) repeatedly by parts, making use of the identity

$$\int \frac{1}{L^2+t^2}\left(\frac{L-it}{L+it}\right)^n dt = \frac{i}{2Ln}\left(\frac{L-it}{L+it}\right)^n + \text{constant}, \qquad n \neq 0. \tag{12}$$

This establishes that for *all* positive integers k

$$a_n = O(n^{-k}), \qquad n \to \infty.$$

Also, for each z in the upper half-plane we have $\frac{\sigma_n(t)}{z-t} \in L_2(\mathbb{R}; W(t))$. Therefore term-by-term integration is allowed in (6), and we conclude that the expansion (7) is valid.

All that remains is the evaluation of the integrals (8). Using residues we find that

$$\frac{i}{\pi}\int_{-\infty}^{\infty}\frac{1}{L^2+t^2}\left(\frac{L+it}{L-it}\right)^n\frac{1}{z-t}\,dt=\begin{cases}\frac{1}{L}\frac{1}{L-iz}, & n=0,\\ \frac{2}{L^2+z^2}\left(\frac{L+iz}{L-iz}\right)^n, & n>0,\\ 0, & n<0.\end{cases}$$

From (7) we thus obtain the expansion

$$w(z)=\frac{1}{\sqrt{\pi}(L-iz)}+\frac{2}{L^2+z^2}\sum_{n=1}^{\infty}a_n\left(\frac{L+iz}{L-iz}\right)^n,\qquad \mathrm{Im}(z)>0, \tag{13}$$

where we have used the fact that $a_0=\frac{L}{\pi}\int_{-\infty}^{\infty}e^{-t^2}\,dt=L/\sqrt{\pi}$.

We draw attention to two useful properties of the expansion (13). First, one readily derives the asymptotic behavior $w(z)\sim i\pi^{-1/2}z^{-1}$ for large $|z|$. Second, by using (12) it is straightforward to integrate (13) term by term to obtain an expansion for $\int_0^z w(\zeta)\,d\zeta$; see [33] for details.

To extend the domain of the series (13) to the real line we insert (5) into (4). Evaluating the principal value integral using residues and contours indented at the singularity $t=x$, one concludes that the validity of the series (13) extends to $z=x\in\mathbb{R}$, provided $w(x)$ is interpreted as in (4).

In practice the series (13) is truncated at $n=N$. We need to determine the accuracy in such an approximation, and we need to find the parameter L that maximizes the accuracy for a given N. This depends of course on the behavior of a_n as $n\to\infty$, which is the topic of the next two sections.

3. Recurrence relations. Here we derive recurrence relations for the coefficients a_n. These relations are potentially useful for asymptotic estimates, as well as for numerical computation. As we shall argue in later sections, however, it may be more efficient to calculate the a_n directly from the integral (11). This remark applies to both the asymptotic calculation (discussed in §4), as well as the numerical calculation (discussed in §6). The results of this section are therefore not essential to the rest of the paper. We decided to include them, nevertheless, since (a) analytical formulas for the expansion coefficients are derived (admittedly of questionable practical value), and (b) interesting connections with other expansions in the literature are obtained.

Consider the expansions

$$(L^2+t^2)e^{-t^2}=\sum_{n=-\infty}^{\infty}a_ne^{in\theta}\quad\text{and}\quad e^{-t^2}=\sum_{n=-\infty}^{\infty}c_ne^{in\theta}, \tag{14}$$

where $t=L\tan\frac{1}{2}\theta$ (recall (10)). The a_n are the expansion coefficients of (13), and the c_n are the coefficients of an alternative expansion introduced in §5. Using the identity

$$\frac{1}{L^2+t^2}=\frac{1}{2L^2}(1+\cos\theta)$$

one deduces that

$$4L^2c_n=a_{n-1}+2a_n+a_{n+1}. \tag{15}$$

Recurrence relations for the c_n may be obtained by exploiting the fact that $f(t)=e^{-t^2}$ satisfies the differential equation

$$f'(t)+2tf(t)=0.$$

Inserting (14), and using trigonometric identities, it is possible to show that

$$nc_n + \left[3(n+1) - 4L^2\right] c_{n+1} + \left[3(n+2) + 4L^2\right] c_{n+2} + (n+3)c_{n+3} = 0. \tag{16}$$

Interestingly, this is precisely the recurrence studied in [34, pp. 125–126]. Using the techniques described there, it is possible to compute the c_n, after which the a_n can be obtained from (15). An alternative approach is to exploit the connection with Fourier series and use the FFT to compute the a_n or c_n. This will be discussed in §6.

As for asymptotic behavior, the Birkhoff theory of difference equations was used in [34, p. 126] to show that $c_n = O\left(\exp\left[-\frac{3}{2}(Ln)^{3/2}\right]\right)$ as $n \to \infty$. We arrive at the same conclusion in §5 by estimating an integral formula for c_n.

It is also possible to express the coefficients a_n and c_n in terms of Meijer's G-function. In the second expansion in (14) we use the fact that $c_{-n} = c_n$ to obtain

$$e^{-t^2} = c_0 + 2\sum_{n=1}^{\infty} c_n \cos n\theta. \tag{17}$$

Upon defining $y = \frac{1}{2}(1 + \cos\theta)$, and using elementary trigonometry, we get

$$\cos\theta = \frac{L^2 - t^2}{L^2 + t^2} = 2y - 1.$$

Inserting this into (17) gives

$$e^{L^2} e^{-L^2/y} = c_0 + 2\sum_{n=1}^{\infty} c_n T_n(2y-1), \qquad 0 \le y \le 1,$$

where $T_n(\cos\theta) = \cos(n\theta)$ denotes the Chebyshev polynomial of degree n. Disregarding the factor e^{L^2}, this is the expansion studied in [34, pp. 125–126] in connection with the recurrence relation (16). Quoting from this reference we conclude that

$$c_n = \pi^{-1/2} e^{L^2} G_{23}^{30}\left(L^2 \,\middle|\, \begin{matrix} 1-n, & & n+1 \\ 1, & \frac{1}{2}, & 0 \end{matrix}\right), \qquad n > 0.$$

A similar formula for the a_n can be derived, but we skip the details. Perhaps these formulas are of academic interest only.

4. Asymptotic estimates. To estimate the asymptotic behavior of the coefficients a_n one could use the G-function representation or the recurrence relations alluded to in the previous section. However, we choose to derive the asymptotics directly from the integral representation (11), using a steepest descent approach. This approach makes clear the role of the parameter L, allowing us to select it optimally. For a general discussion of the method of steepest descent we refer to [25], [35].

The integral (11) may be written as

$$\frac{\pi}{2L} a_n = \mathrm{Re}\left[\int_0^{\infty} e^{h(t;n)}\, dt\right] = \mathrm{Re}\left[\int_{\Gamma} e^{h(z;n)}\, dz\right], \tag{18}$$

where

$$h(z;n) = -z^2 - 2in \tan^{-1}\tfrac{z}{L}. \tag{19}$$

We have used the Cauchy theorem, which allows us to deform the path of integration $t \in [0, \infty)$ into $z \in \Gamma$ as long as we avoid the branch cuts of the arctangent, which are chosen as those sections of the imaginary axis with $|\mathrm{Im}(z)| > L$.

To make a specific choice for Γ, we look for the saddle points of (19) and calculate

$$h'(z) = -2z - \frac{2iLn}{L^2 + z^2}.$$

Here, and below, we suppress the parametric dependence of h on n. Setting $h'(z) = 0$ shows the saddle points $z = z_s$ to be given by

$$z_s^3 + L^2 z_s + iLn = 0. \tag{20}$$

Since both n and L are positive, one root of this equation is located on the positive imaginary axis and the other two are in the lower half-plane. For small n, these two roots are on the negative imaginary axis, but as n increases they move into the third and fourth quadrants. The root in the fourth quadrant is the relevant saddle point. Solving (20) with $n \to \infty$ while keeping L fixed we find that

$$z_s = e^{-\pi i/6}(Ln)^{1/3} - \tfrac{1}{3}L^2 e^{\pi i/6}(Ln)^{-1/3} + O(n^{-5/3}). \tag{21}$$

We can now make a definite choice for Γ: it consists of the three parts shown in Fig. 1(a). Γ_1 is that part of the imaginary axis between the origin and $-i(L-\delta)$, where δ is a small positive number. Γ_3 is the steepest descent path $\mathrm{Im}\,[h(z)] = \text{constant}$, or, writing $z = x + iy$,

$$\Gamma_3 : -2xy - n\tan^{-1}\left[\frac{2Lx}{L^2 - y^2 - x^2}\right] = \text{constant}. \tag{22}$$

The constant is chosen such that the path passes through the saddle point $z = z_s$ defined above. Γ_2 is a small circular arc connecting Γ_1 and Γ_3; it has center $z = -iL$ and radius $\delta (\ll L)$.

On Γ_1 the integral in (18) is pure imaginary, therefore we ignore this contribution. On Γ_2 the integral is vanishingly small in the limit $\delta \to 0$, as can be seen from the estimate

$$\left| \int_{\Gamma_2} e^{-z^2} \left(\frac{L - iz}{L + iz}\right)^n dz \right| \le \pi\delta e^{(L+\delta)^2} \left(\frac{\delta}{2L - \delta}\right)^n,$$

obtained by using the bounds

$$|e^{-z^2}| \le e^{(L+\delta)^2}, \quad |L + iz| \ge 2L - \delta, \quad \int_{\Gamma_2} |dz| \le \pi\delta, \quad z \in \Gamma_2.$$

That leaves us with estimating the integral on Γ_3. The main contribution comes from the neighborhood of the saddle point $z = z_s$, and so we use (21) to calculate

$$\begin{aligned}
z_s^2 &= e^{-\pi i/3}(Ln)^{2/3} - \tfrac{2}{3}L^2 + O(n^{-2/3}),\\
2in\tan^{-1}\tfrac{z_s}{L} &= \pi in - 2ie^{\pi i/6}(Ln)^{2/3} + \tfrac{2}{3} + O(n^{-2/3}),\\
h(z_s) &= -i\pi n + \tfrac{3}{2}(3^{1/2}\,i - 1)(Ln)^{2/3} + \tfrac{2}{3}L^2 + O(n^{-2/3}),\\
h''(z_s) &= -6 + O(n^{-2/3}),\\
h^{(k)}(z_s) &= O(n^{(4-2k)/3}), \qquad k = 3, 4, \ldots.
\end{aligned}$$

Approximating $h(z)$ with a Taylor expansion centered at $z = z_s$ yields

$$\begin{aligned}\int_\Gamma e^{h(z)}\,dz &\sim e^{h(z_s)}\int_{\Gamma_3} e^{(1/2)h''(z_s)(z-z_s)^2}\,dz \\ &\sim (-1)^n e^{-(3/2)(Ln)^{2/3}} e^{(2/3)L^2} e^{i(3^{3/2}/2)(Ln)^{2/3}} \left(\frac{\pi}{3}\right)^{1/2},\end{aligned} \tag{23}$$

where we approximated

$$\int_{\Gamma_3} e^{(1/2)h''(z_s)(z-z_s)^2}\,dz \sim \int_{\Gamma_3} e^{-3(z-z_s)^2}\,dz \sim \int_{-\infty}^{\infty} e^{-3x^2}\,dx = \left(\frac{\pi}{3}\right)^{1/2}$$

in the usual manner. Substituting (23) into (18) yields, as $n \to \infty$,

$$a_n \sim (-1)^n 2L(3\pi)^{-1/2} e^{(2/3)L^2} \cos\left[\left(\tfrac{3^{3/2}}{2}\right)(Ln)^{2/3}\right] \exp\left[-(\tfrac{3}{2})(Ln)^{2/3}\right]. \tag{24}$$

This estimate is very accurate, even for small n, as is confirmed numerically in Fig. 3(a).

The above analysis is also useful for estimating the optimal value of the parameter L. A naive look at (24) suggests that by increasing L, the asymptotic decay rate in the coefficients can be increased unboundedly. That is true, but in a practical application the series (13) is truncated at a finite point, say, at $n = N$. Choosing L too large results in a decreased convergence rate, on average, over the first N coefficients. This can be seen in Fig. 2(a), where we plot the coefficients $|a_n|$ for various values of L. A different perspective is shown in Fig. 2(b), where we depict the level curves of $|a_N|$ as a function of N and L. We need to find the relationship between L and N that will take us down the middle of the valley, as indicated by the dashed curve.

To estimate the optimal relationship L versus N, we adapt an idea of Boyd [1], which was used to estimate optimal mapping parameters in Chebyshev approximations on the real line. We need to determine L as a function of N such that the coefficient

$$a_N = \frac{L}{\pi}\int_{-\infty}^{\infty} e^{-t^2}\left(\frac{L-it}{L+it}\right)^N dt \tag{25}$$

decays as rapidly as possible when $N \to \infty$.

A steepest descent treatment of the integral leads as before to (20), with N replacing n, and L is no longer constant but a function of N. The decay of a_N is determined by $\mathrm{Re}[h(z_s)]$. Asymptotic balancing of the terms in (20) shows that $\mathrm{Re}[h(z_s)] = O(N)$ (that is, geometric decay in a_N) can be achieved only if $L \propto N^{1/2}$. That prompts us to make the change of variables

$$z = \zeta N^{1/2}, \qquad L = \lambda N^{1/2}, \tag{26}$$

transforming (18) into

$$a_N = \frac{2\lambda N}{\pi}\mathrm{Re}\left[\int_\Gamma e^{-g(\zeta)N}\,d\zeta\right], \tag{27}$$

where

$$g(\zeta) = \zeta^2 + 2i\tan^{-1}(\tfrac{\zeta}{\lambda}).$$

The saddle points are given by $g'(\zeta_s) = 0$, i.e.,

$$\zeta_s^3 + \lambda^2 \zeta_s + i\lambda = 0. \tag{28}$$

Again there is one root ζ_s located on the positive imaginary axis and two in the lower half-plane. For large λ they are located on the negative imaginary axis. The one nearest to the origin satisfies $-\lambda < \mathrm{Im}(\zeta_s) < 0$ and is the relevant saddle point. For small λ the two roots are located in the third and fourth quadrants; the latter one is the relevant saddle point. In either case a steepest descent analysis can in principle be carried out as before. The crucial observation is that the decay in a_N is determined by $\mathrm{Re}[g(\zeta_s)]$.

We are thus faced with the scalar optimization problem: Find $\lambda \in \mathbb{R}$ such that

$$\mathrm{Re}[g(\zeta_s)] = \text{maximum},$$

where $\zeta_s = \zeta_s(\lambda)$ is implicitly defined by (28). The solution of this problem is $\mathrm{Re}[\frac{dg}{d\lambda}] = 0$, and using the chain rule we calculate

$$\frac{dg}{d\lambda} = \frac{\partial g}{\partial \zeta_s}\frac{\partial \zeta_s}{\partial \lambda} + \frac{\partial g}{\partial \lambda}.$$

The first term on the right vanishes since $\partial g/\partial \zeta_s = 0$ is the defining equation for the saddle point (28). Hence

$$\frac{dg}{d\lambda} = \frac{\partial g}{\partial \lambda} = \frac{2i\zeta_s}{\lambda^2 + \zeta_s^2},$$

and equating the real part to zero gives $\lambda = |\zeta_s|$. Setting $\zeta_s = \lambda e^{i\alpha}$ in (28) yields a complex equation for the unknown real variables λ and α. The real part of this equation yields $\alpha = -\frac{\pi}{4}$, and from the imaginary part we get $\lambda = 2^{-1/4}$. Thus the optimal choice is

$$L = 2^{-1/4} N^{1/2}.$$

We have indicated this relationship with the dashed line in Fig. 2(b), confirming the validity of the estimate.

Having established the optimal relationship between L and N, we can now complete the steepest descent analysis of (27) to determine the decay in a_N as $N \to \infty$. The contour of integration is shown in Fig. 1(b). The contributions along the paths Γ_1 and Γ_2 are ignored, as in the previous analysis. The steepest descent path Γ_3 can be obtained from (22) after making the change of variables (26). The main contribution along this contour comes from the neighborhood of the saddle point $\zeta_s = 2^{-1/4} e^{-\pi i/4}$, and so we calculate

$$g(\zeta_s) = -\log(2^{1/2} - 1) + i(\tfrac{\pi}{2} - 2^{-1/2}), \qquad g''(\zeta_s) = 4 - 2i.$$

Approximating $g(\zeta)$ near $\zeta = \zeta_s$, using a Taylor series up to terms in $(\zeta - \zeta_s)^2$, yields

$$\int_{\Gamma_3} e^{-g(\zeta)N}\, d\zeta \sim e^{-g(\zeta_s)N} \int_{\Gamma_3} e^{-(1/2)g''(\zeta_s)(\zeta-\zeta_s)^2 N}\, d\zeta. \tag{29}$$

The integral on the right-hand side is estimated in the standard way, by writing $\frac{1}{2}g''(\zeta_s) = 2 - i = 5^{1/2} e^{-i\beta}$, where $\beta = \tan^{-1}\frac{1}{2}$, and parametrizing the path near

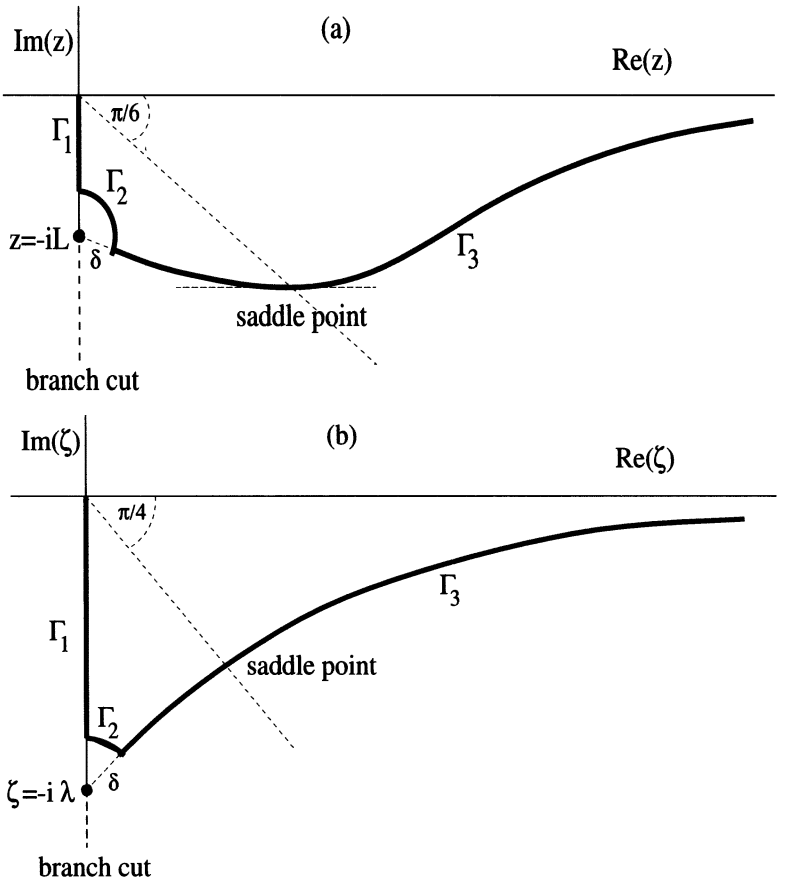

FIG. 1. *Schematic representation of the contours of integration for the asymptotic estimate of* (a) *the integral* (18), *and* (b) *the integral* (27).

$\zeta = \zeta_s$ as $\zeta - \zeta_s = te^{i\beta/2}$. Arguing that the limits on t can be extended to $\pm\infty$, incurring only a negligible error in the process, we obtain

$$\int_{\Gamma_3} e^{-(1/2)g''(\zeta_s)(\zeta-\zeta_s)^2 N}\, d\zeta \sim e^{i\beta/2} \int_{-\infty}^{\infty} e^{-5^{1/2}t^2}\, dt = \left(\frac{\pi}{N}\right)^{1/2} 5^{-1/4} e^{i\beta/2}.$$

Finally, substitution of (29) into (27) yields, as $N \to \infty$,

$$(30)\quad a_N \sim 2^{3/4}5^{-1/4}\left(\frac{N}{\pi}\right)^{1/2} \cos\left[N\left(\frac{1}{2^{1/2}} - \frac{\pi}{2}\right) + \frac{1}{2}\tan^{-1}\frac{1}{2}\right]\left[2^{1/2}-1\right]^N.$$

We offer Fig. 3(b) as numerical verification of this formula.

The above results enable us to estimate the truncation error in (13), defined by

$$E_N(z) = \frac{2}{L^2+z^2} \sum_{n=N+1}^{\infty} a_n \left(\frac{L+iz}{L-iz}\right)^n.$$

The coefficients a_n decay relatively fast (compare (24)) and therefore the first omitted term should at least provide an order-of-magnitude estimate of the truncation error.

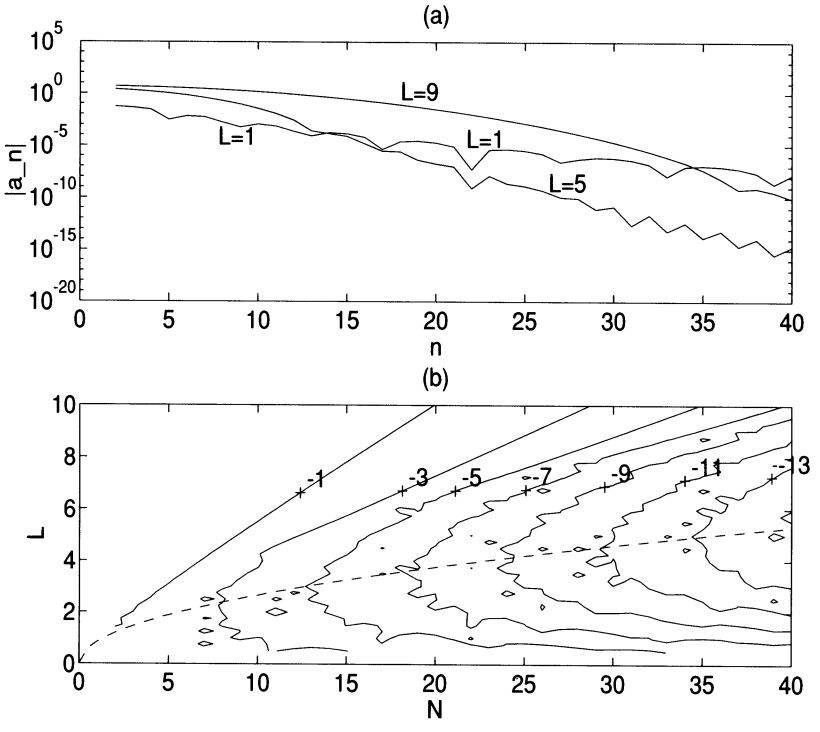

FIG. 2. (a) *The coefficients* $|a_n|$, *defined by* (11), *for* $L = 1, 5, 9$. (b) *Level curves of the quantity* $|a_N|$ *as a function of* N *and* L. *The label* t *indicates that* $|a_N| = 10^t$ *on that curve. The dashed line represents the optimal relationship* $L = 2^{-1/4}N^{1/2}$.

Estimating from (30) that $|a_{N+1}| \approx (N+1)^{1/2}[2^{1/2}-1]^{N+1}$, one obtains

$$|E_N(z)| \approx 2(N+1)^{1/2}(2^{1/2}-1)^{N+1}\frac{1}{|L^2+z^2|}\left|\frac{L+iz}{L-iz}\right|^{N+1}. \tag{31}$$

Observe that for large $|z|$, as well as for $z \approx iL$, $|E_N(z)|$ is small, even for moderate N. This is confirmed in Fig. 4.

A nonrigorous bound, applicable to all z in the upper half-plane, can be obtained by using the inequalities $|\frac{L+iz}{L-iz}| \le 1$ and $|L-iz|^{-1} < L^{-1}$ to get

$$|E_N(z)| \le 2^{3/2}(2^{1/2}-1)^{N+1}.$$

For example, for $N = 8$ and $N = 16$ this suggests that $|E_N(z)| \le 10^{-2.6}$ and $|E_N(z)| \le 10^{-5.7}$, respectively, uniformly for z in the upper half-plane. This correlates well with the results given in Fig. 4, except of course in the regions $|z|$ large, and $z \approx iL$. (Note that we have plotted relative errors in Fig. 4, not absolute (= truncation) errors. However, since $w(z)$ has the property that both its real and imaginary parts are between zero and one in the first quadrant, the results in Fig. 4 should also give an indication of the truncation error.)

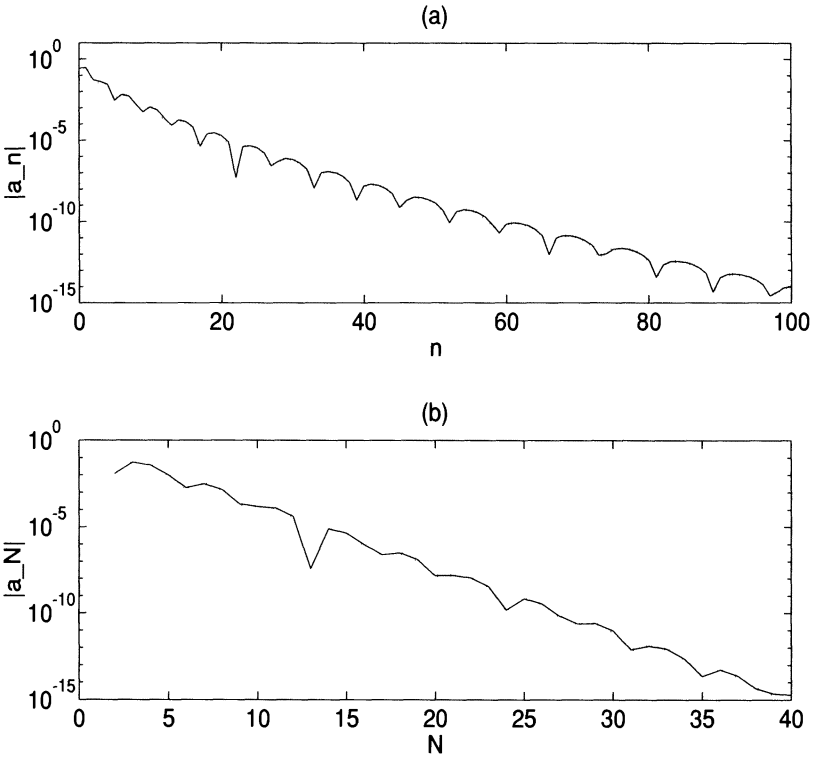

FIG. 3. (a) *Comparison of the estimate* (24) *with the true values of* a_n *for* $L = 1$. (b) *Comparison of the estimate* (30) *with the true values of* a_N *for* $L = 2^{-1/4}N^{1/2}$. *The circles represent the asymptotic estimates and the true values (as computed accurately with the* FFT; *see* §6) *are connected by continuous line segments.*

5. Alternative expansions. Another set of basis functions that may be used as an alternative to (9) is defined by

$$\rho_n(t) = \frac{1}{L-it}\sigma_n(t) = \frac{1}{L-it}\left(\frac{L+it}{L-it}\right)^n. \qquad \text{basis for Im(z)=0}$$

These functions are complete and orthogonal in $L_2(\mathbb{R}; W(t))$ with weight function $W(t) = 1$.

Following the same procedure as in §2, one considers the expansion

$$e^{-t^2} = \sum_{n=-\infty}^{\infty} b_n\rho_n(t), \quad \text{with } b_n = \frac{L}{\pi}\int_{-\infty}^{\infty}\frac{e^{-t^2}}{L+it}\left(\frac{L-it}{L+it}\right)^n dt. \tag{32}$$

Substitution into (5)–(7) yields

$$w(z) = \frac{2}{L-iz}\sum_{n=0}^{\infty} b_n\left(\frac{L+iz}{L-iz}\right)^n. \tag{33}$$

The coefficients b_n decay slightly faster than the coefficients a_n studied earlier. In particular, the analysis of §4 can be modified to obtain

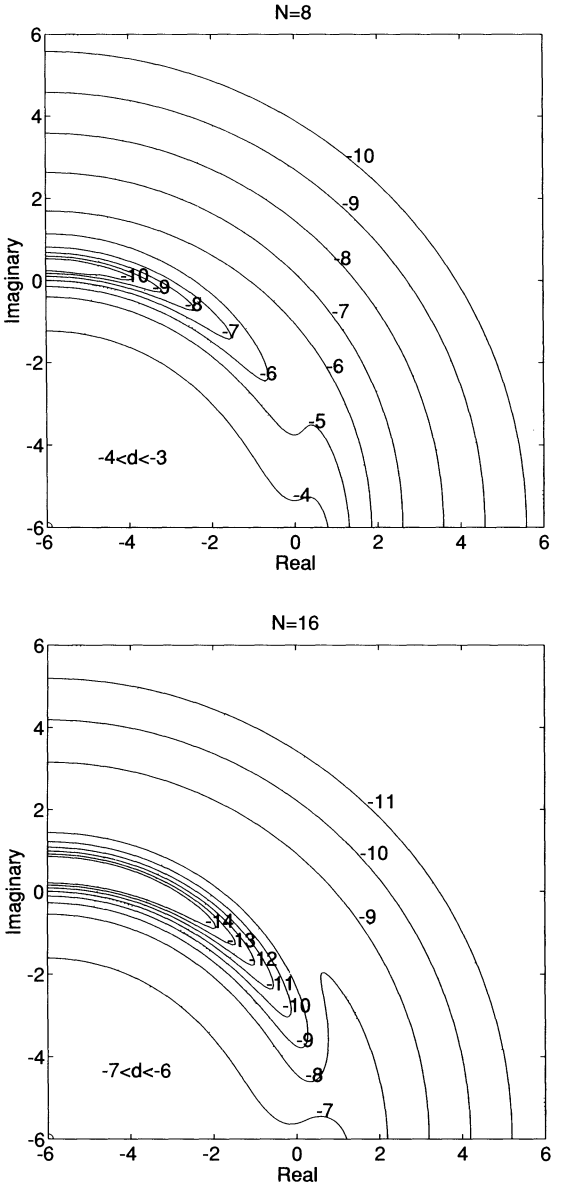

FIG. 4. *Level curves of the relative error in the expansion* (I); *see* (38). *The label d on each curve indicates that the relative error is of magnitude* 10^d *there. The label on the coordinate axes refers to p, where* $z = 10^p e^{i\theta}$.

$$b_n \sim (-1)^n 2L^{2/3} m^{-1/3} (3\pi)^{-1/2} e^{(2/3)L^2} \cos\left[\left(\tfrac{3^{3/2}}{2}\right)(Lm)^{2/3} + \tfrac{5\pi}{3}\right] \times \exp\left[-\left(\tfrac{3}{2}\right)(Lm)^{2/3}\right],$$

where $m = n + \frac{1}{2}$. This reveals a factor of $O(n^{-1/3})$ in the coefficient, and a phase shift in the cosine term, not present in (24). This is a consequence of the factor

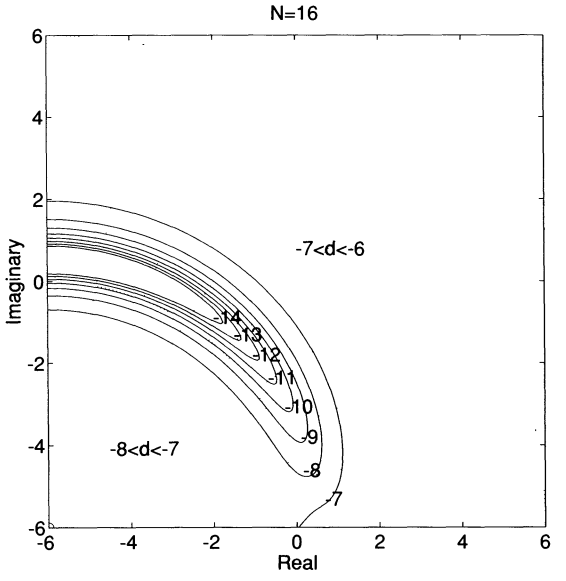

FIG. 5. *Same as Fig.* 4, *but based on the expansion* (II); *see* (38).

$(L + it)^{-1}$ in the integrand of (32). The optimal value of L can be estimated as in §4, and again it is found to be $L = 2^{-1/4}N^{1/2}$. With this choice of L, it follows that $b_N = O((2^{1/2} - 1)^N)$, akin to (30).

The quicker decay of the b_n compared to the a_n suggests that the expansion (33) is better for computational purposes than (13). This is only true for small $|z|$, and even then the improvement is slight. When truncated, the series (13) has a remainder of magnitude $O(|z|^{-2})$, compared to $O(|z|^{-1})$ in (33). Therefore we expect our earlier expansion to be significantly superior as $|z| \to \infty$. We compare the two expansions numerically in Figs. 4 and 5.

Yet another possibility is to use the second expansion in (14) rather than the first. That is, consider

$$e^{-t^2} = \sum_{n=-\infty}^{\infty} c_n \sigma_n(t), \quad \text{with } c_n = \frac{L}{\pi} \int_{-\infty}^{\infty} \frac{e^{-t^2}}{L^2 + t^2} \left(\frac{L - it}{L + it} \right)^n dt. \tag{34}$$

When this expansion is inserted into the integral representation (3), a technical problem arises: The integrals $\int_{-\infty}^{\infty} \sigma_n(t)(z - t)^{-1}\, dt$ do not converge in the normal sense. A quick remedy is to modify (3) to

$$w(z) = \frac{iz}{\pi} \int_{-\infty}^{\infty} \frac{e^{-t^2}}{z^2 - t^2}\, dt, \qquad \mathrm{Im}(z) > 0. \tag{35}$$

When (34) is inserted, all integrals converge, and one obtains

$$w(z) = c_0 + 2 \sum_{n=1}^{\infty} c_n \left(\frac{L + iz}{L - iz} \right)^n. \tag{36}$$

In this expansion the coefficients c_n decay most rapidly of all, gaining yet another factor of $O(n^{-1/3})$ on the coefficients b_n:

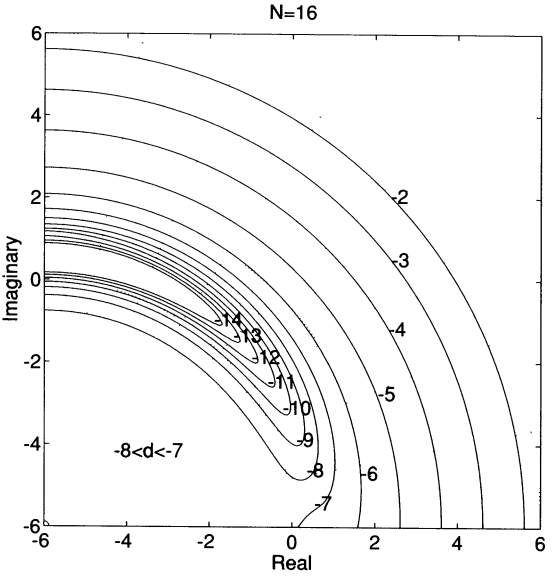

FIG. 6. *Same as Figs.* 4–5, *but based on the expansion* (III); *see* (38).

(37)
$$c_n \sim (-1)^n 2L^{1/3} n^{-2/3} (3\pi)^{-1/2} e^{(2/3)L^2} \cos\left[\left(\tfrac{3^{3/2}}{2}\right)(Ln)^{2/3} + \tfrac{\pi}{3}\right] \times \exp\left[-\left(\tfrac{3}{2}\right)(Ln)^{2/3}\right].$$

When truncated, however, the accuracy of the expansion (36) deteriorates rapidly as $|z|$ grows large (see Fig. 6). We recall that the leading behavior in (37) was obtained in [34, p. 126] through a local analysis of the difference equation (15).

6. Implementation and tests. In this section we discuss the implementation of the three expansions derived in this paper, and we compare them numerically. For easy reference we label them as (I)–(III), where

(38)
$$\text{(I)} \quad w(z) \approx \frac{1}{\sqrt{\pi}(L - iz)} + \frac{2}{(L - iz)^2} \sum_{n=0}^{N-1} a_{n+1} Z^n,$$
$$\text{(II)} \quad w(z) \approx \frac{2}{L - iz} \sum_{n=0}^{N} b_n Z^n,$$
$$\text{(III)} \quad w(z) \approx c_0 + 2 \sum_{n=1}^{N} c_n Z^n.$$

In all cases
$$Z = \frac{L + iz}{L - iz}, \quad \text{and} \quad L = 2^{-1/4} N^{1/2}.$$

The first series was rewritten in the stated form to minimize the loss of significance error when $z \approx iL$ (compare (13)).

TABLE 1
Matlab program for computing $w(z) = e^{-z^2}\,erfc(-iz)$ *using the series* (I).

```
function w = cef(z,N)

% Computes the function w(z) = exp(-z^2) erfc(-iz) using a rational
% series with N terms. It is assumed that Im(z) > 0 or Im(z) = 0.

M = 2*N; M2 = 2*M; k = [-M+1:1:M-1]';   % M2 = no. of sampling points.
L = sqrt(N/sqrt(2));                    % Optimal choice of L.
theta = k*pi/M; t = L*tan(theta/2);     % Variables theta and t.
f = exp(-t.^2).*(L^2+t.^2); f = [0; f]; % Function to be transformed.
a = real(fft(fftshift(f)))/M2;          % Coefficients of transform.
a = flipud(a(2:N+1));                   % Reorder coefficients.
Z = (L+i*z)./(L-i*z); p = polyval(a,Z); % Polynomial evaluation.
w = 2*p./(L-i*z).^2+(1/sqrt(pi))./(L-i*z);  % Evaluate w(z).
```

We discuss only the implementation of (I), since (II) and (III) may be implemented similarly. Computing the coefficients a_n can be done through recurrence relations as discussed in §3. We feel the most practical approach, however, is to compute the coefficients directly from the integral (11). After making the change of variable $t = L\tan\frac{1}{2}\theta$, we apply the trapezoidal rule with $2M$ gridpoints, where $M \gg N$. This yields approximations $A_n \approx a_n$, where

$$A_n = \frac{1}{2M}\sum_{j=-M+1}^{M-1}(L^2 + t_j^2)e^{-t_j^2}e^{-in\theta_j}, \qquad n = 1,\dots,N \tag{39}$$

with

$$t_j = L\tan\frac{1}{2}\theta_j, \quad \theta_j = \frac{\pi j}{M}, \quad j = -M+1,\dots,M-1.$$

This is a discrete Fourier transform and computable with one FFT, rather than N separate summations. The errors in A_n can be expressed as [16, p. 19]

$$A_n - a_n = \sum_{k=1}^{\infty} a_{n\pm 2kM}.$$

Recalling the asymptotic estimate (24), we conclude that these errors decay swiftly as $M \to \infty$ with n fixed. In practice we found that using $M = 2N$ in (39) is sufficient to ensure that the error incurred by using A_n instead of a_n is on the same order of magnitude as the truncation error in (I).

Once the coefficients are calculated, (I) may be evaluated with the Horner algorithm. The Matlab program in Table 1 implements the method. A few comments are in order:

- The program assumes that z is in the upper half-plane. For values in the lower half-plane the formula $w(-z) = 2e^{-z^2} - w(z)$ may be used, but one should be aware of possible loss of accuracy due to cancellation. This occurs near the zeros of $w(z)$ (see [26]).
- If $z = x \in \mathbb{R}$, the real and imaginary parts of $w(x)$ return approximations to e^{-x^2} and $(2/\sqrt{\pi})\mathrm{daw}(x)$, respectively, as indicated by (4).

- For $N = 16$, the program delivers six significant decimal digits, or better, for z in the upper half-plane (see Fig. 4). For $N = 32$ this improves to about twelve digits.
- The program takes advantage of Matlab's built-in vector operations. The input argument z may be a vector or a matrix.

Using programs such as these we compared the accuracy of the expansions (I)–(III). We computed the values of $w(z)$ for $z = 10^p e^{i\theta}$, for $p = -6(0.06)6$, and $\theta = 0(\frac{\pi}{400})\frac{\pi}{2}$, i.e., $201^2 = 40401$ values in total. The relative error in each approximation was calculated using Algorithm 680 of the ACM (discussed in the next section), which computes $w(z)$ accurately to at least 14 significant digits. Matlab's working precision is about 16 digits. The results were processed by Matlab's contour plotting routine, and are shown in Figs. 4–6. The label d on the level curves provides an indication of the number of correct digits.

We confirm some earlier predictions regarding the accuracy in Figs. 4–6. First, note that all three expansions give exceptional accuracy near $z = iL$. This is fortunate, since $z = iy$ corresponds to the computation of the important function $e^{y^2}\operatorname{erfc}(y)$. Second, for small $|z|$, (III) is better than (II), which, in turn, is better than (I). This was predicted in §5 based on an examination of the decay rate of the expansion coefficients. Third, for large $|z|$, expansion (I) is significantly superior to (II) with (III) failing badly. We predicted this in §5 by noting that the truncation errors are $O(|z|^{-2})$, $O(|z|^{-1})$, and $O(1)$, respectively, as $|z| \to \infty$. For overall performance our vote goes to (I).

There is a strategy for further improving the efficiency. When $z = iy$, (I)–(III) are power series of a real variable—this calls for Lanczos economization. Take (I) as example, and consider the representation

$$\sum_{n=0}^{N-1} a_{n+1} Z^n = \sum_{n=0}^{N-1} d_{n+1} T_n(Z)$$

with T_n denoting the Chebyshev polynomial of degree n. It is possible to compute the coefficients d_n in terms of the a_n using the methods described in [19], for example. In general, the d_n decay quickly compared to the a_n. This allows for a significant improvement in efficiency when Z is real, i.e., when z is pure imaginary. However, when extended into the complex plane the Chebyshev polynomials lose the critical property $|T_n(Z)| \le 1$, $Z \in [-1, 1]$. Fortunately, the magnitude of $T_n(Z)$ for z in most regions of the upper half-plane is not sufficiently large to offset the gain in decay rate of the expansion coefficients. The exception occurs near $z = \pm L$, where $|T_n(Z)|$ assumes its maximum value of $|T_n(i)| \sim \frac{1}{2}(\sqrt{2}+1)^n$.

We used the economization approach in Fig. 7, which should be compared with Fig. 4. Observe the increase in accuracy for most z. Near $z = L$, however, the economization becomes wasteful instead. Unfortunately, this includes the important special case $z \in \mathbb{R}$, $z = O(1)$, which corresponds to the computation of the real-valued Dawson function. But for z away from $z = L$, like the equally important case $z = iy$, $w(z) = e^{y^2}\operatorname{erfc}(y)$, the economization is recommended.

7. Survey and comparison of algorithms. Elementary approximations of the error function abound; a partial list may be found in [18, p. 55]. These methods make no provision for complex arguments, however, and they are of limited accuracy. For higher precision requirements, there seem to be four distinct classes of algorithms:

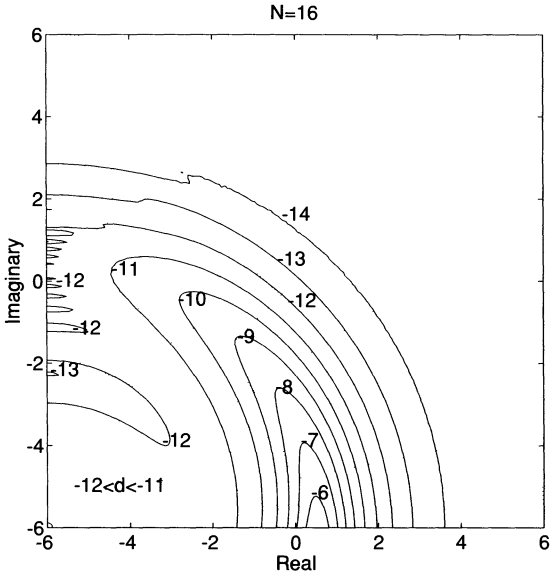

FIG. 7. *Same as Fig.* 4, *but Chebyshev economization is used.*

- The Padé rational approximations of Cody and coworkers (see [4]–[7]), as may be found in the *fn* and *Specfun* libraries available from Netlib [8], as well as in Matlab 4.1 [21].
- Methods based on trapezoidal or midpoint rule approximations of (35) (see [15], [22], [23]).
- The Chebyshev approximations of Clenshaw, Luke, and Schonfelder (see [20, 29]). These methods form the basis of the algorithms in the NAG library [24].
- Continued fractions, used in generating the tables [11], with later refinements by Gautschi [14] and Poppe and Wijers [26]. The latter two approaches are implemented as TOMS Algorithms 363 and 680 of the ACM, respectively. (See [13], [27].) Gautschi's original algorithm is used in the IMSL library [17].

In this section we compare the merits of these approaches with ours.

The Padé approximations discussed in [4]–[7] give high accuracy at low computational cost. As implemented in the libraries referenced above, however, no provision for complex arguments is made. Moreover, the real line must be subdivided in a number of smaller intervals for the algorithm to retain its efficiency. Finding the coefficients is an elaborate procedure, requiring Remez-type algorithms.

The trapezoidal rule applied to the modified integral representation (35) leads to the formula

$$w(z) \approx \frac{ihz}{\pi} \sum_{n=-\infty}^{\infty} \frac{e^{-n^2h^2}}{z^2 - n^2h^2} - R(z;h), \qquad \mathrm{Im}(z) > 0, \tag{40}$$

where $R(z;h)$ is a correction term given in [22], [23], where error estimates are also presented. For the midpoint rule analogue, see [15]. In a practical implementation the

series (40) is truncated to, say, $-N \leq n \leq N$. The formula is very accurate, provided for given z and N the optimal stepsize h is selected. It is not easy, however, to determine this optimal h a priori. By contrast, we were able to determine our optimal parameter $L = 2^{-1/4}N^{1/2}$ independently of z (§4). Moreover, the high accuracy is lost for z near the real axis, even with an optimal h. Further difficulties are that (40) blows up when $z = nh$ for some integer n and that it is unstable for values $z \approx nh$. These drawbacks may be to blame for the fact that the trapezoidal/midpoint methods have not found their way into the software libraries.

Another class of highly accurate methods are the rational Chebyshev approximations of Schonfelder, based on earlier work of Luke and Clenshaw (see [20], [29]). Our expansions are closely related to these. In particular, Schonfelder discusses the expansion [29]

$$e^{x^2}\operatorname{erfc}(x) = \sum_{n=0}^{N} a_n T_n(t), \qquad t = \frac{x-k}{x+k}, \tag{41}$$

which forms the basis for the complementary error function routine S15ADF in the NAG library [24]. Comparing this with our expansion (III) (see (38)), one concludes that (41) may be viewed as an economized version of (III) with L and k playing equivalent roles. In a certain sense the present work may therefore be considered an extension of that of Clenshaw, Luke, and Schonfelder. First, we showed how to extend these expansions to complex arguments—no mention of complex variables is made in [20], [29], and the NAG implementation of (41) does not make provision for them [24]. Second, we improved (41) significantly for large x, sacrificing only a nominal degree of accuracy for small x—compare (I) with (III) and (41), as well as Fig. 4 with Fig. 6. Third, we showed how the expansion coefficients can be computed via the FFT—by contrast these coefficients were obtained in [29] through a laborious procedure, both in terms of computational cost and human effort. Fourth, we were able to estimate the parameter L theoretically—in [29] the proposed value of $k = 3.75$ was arrived at empirically.

Another efficient method is based on the continued fraction [11], [14]

$$w(z) = \frac{i}{\sqrt{\pi}} \frac{1}{z-} \frac{\frac{1}{2}}{z-} \frac{1}{z-} \frac{\frac{3}{2}}{z-} \cdots. \tag{42}$$

When truncated, this formula yields high accuracy, but only for large $|z|$. For small $|z|$, Gautschi [14] proposed the use of Taylor expansions with coefficients computed by continued fractions. This forms the basis of TOMS Algorithm 363 [13] and the algorithm CERFE/ZERFE in the IMSL library [17]. Further improvements of this algorithm were suggested in [26] and can be found implemented as TOMS Algorithm 680 [27]. A closely related algortithm is the Fortran code given in [30], which, in addition to the continued fraction, also uses the asymptotic expansion of $w(z)$ for large z.

A comparison of our expansions with Algorithm 680 is not a fair test, since this is a finely tuned piece of software, using various expansions to achieve fourteen digit accuracy uniformly in the first quadrant. By contrast, our method is based on a single expansion. As such it should be compared to Taylor expansions or continued fractions. Nevertheless, we found that there is some region in the first quadrant in which our expansion is indeed competitive with Algorithm 680.

To compare efficiencies, we have to sketch the details of Algorithm 680 briefly. The first quadrant is subdivided into three regions, S, R, and Q, separated by the thicker

ellipses shown in Fig. 8. These ellipses are defined by $\varrho(z) = 0.292$ and $\varrho(z) = 1$, respectively, where

$$\varrho(z) = \sqrt{(x/x_0)^2 + (y/y_0)^2}, \quad z = x + iy, \quad x_0 = 6.3, \quad y_0 = 4.4.$$

Attention is restricted to the first quadrant only, since values of $w(z)$ in the other quadrants can be obtained from those in the first by elementary relations (see [26]).

In the inner region S the Taylor polynomial is used

$$w(z) \approx e^{-z^2}\left(1 + \frac{2i}{\sqrt{\pi}} \sum_{n=0}^{N} \frac{z^{2n+1}}{(2n+1)n!}\right)$$

with degree

$$N = \left\{6 + 72\left(1 - 0.85\frac{y}{y_0}\right)\varrho(z)\right\}. \tag{43}$$

Here, and below, the symbol { } denotes rounding.

In the outer region Q, the νth convergent of the continued fraction (42) is used, where

$$\nu = \left\{3 + \frac{1442}{26\varrho(z) + 77}\right\}. \tag{44}$$

In the intermediate region R a Taylor expansion is used, where the coefficients are computed by continued fractions (for details, see [26]). The degree of the polynomial is N, and the continued fraction calculation involves ν convergents, where

$$N = \{7 + 34\, s(z)\}, \qquad \nu = \{16 + 26\, s(z)\}, \tag{45}$$

and

$$s(z) = \left(1 - \frac{y}{y_0}\right)\sqrt{1 - \varrho^2(z)}.$$

For an operation count, we consider the cost of evaluating a polynomial of degree N equivalent to the cost of evaluating the Nth convergent of a continued fraction. Both involve essentially N additions and N multiplications. Thus we shall use the phrase "degree of approximation" to indicate the degrees of each of these processes. Specifically, the degrees of approximation in the regions S, Q, and R are N, ν, and $N + \nu$, respectively, as defined by (43), (44), and (45). By comparison, the rational expansion is also implemented by evaluating a polynomial. Therefore, we compare efficiencies by simply comparing the degrees of approximation required by each algorithm to achieve a given accuracy (fourteen digits) in various regions of the complex plane.

In the first picture in Fig. 8 we show the degree of approximation used by Algorithm 680, as defined by (43)–(45). The second picture applies to the rational expansion (I): we show the minimum degree of polynomial required to achieve a relative difference of less than $\frac{1}{2}10^{-14}$ compared to the value of $w(z)$ as computed by Algorithm 680. As suggested by the error estimate (31), the curves of constant N are roughly given by the circles $|\frac{L+iz}{L-iz}| = \text{constant}$.

A comparison of the two figures reveals that Algorithm 680 is superior for $|z|$ small and $|z|$ large. The rational expansion is competitive, however, for intermediate values

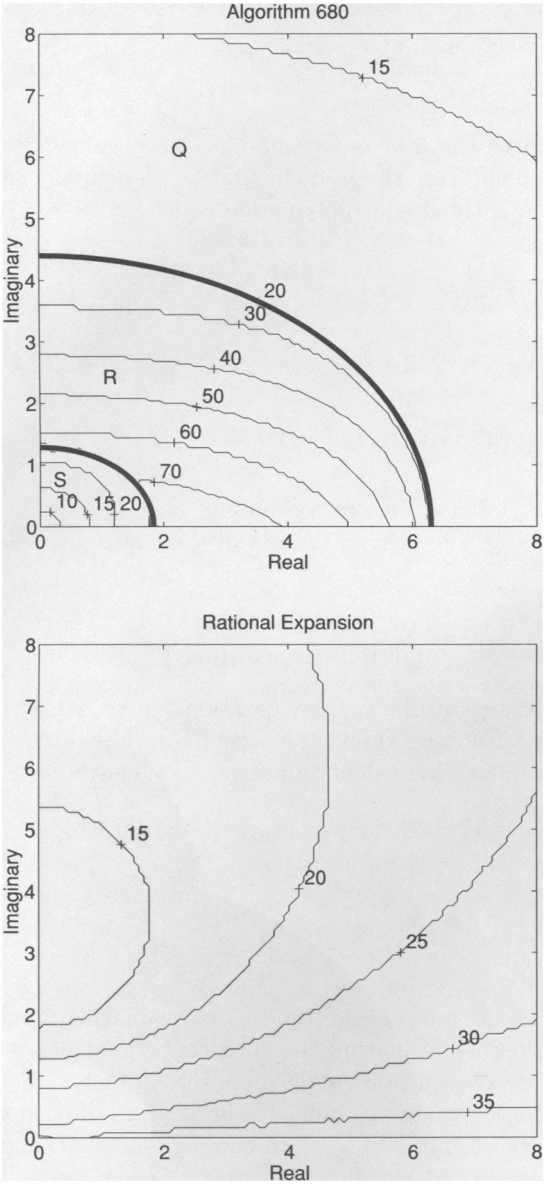

FIG. 8. *The curves show values of z along which a constant degree of approximation is used to compute w(z) to fourteen digits. The shaded region indicates where the rational expansion is competitive. (Note: in these graphs the z variable is not represented on a log-scale, as was the case in Figs. 4–7).*

of $|z|$. Specifically, in the second figure we have shaded the region in which the rational expansion yields the specified accuracy with a polynomial of degree less than the degree of approximation used by Algorithm 680. Of particular interest is the interval $1.84 \leq x \leq 6$ on the real axis, which corresponds to the real-valued Dawson function. Here the rational expansion provides fourteen digit accuracy with a polynomial of

degree about 40, whereas Algorithm 680 uses a degree somewhere between 40 and 80. Likewise, on the imaginary axis, which corresponds to $w(iy) = e^{y^2}\operatorname{erfc}(y)$, the rational expansion proves to be competitive for a sizable range of y values. For example, in the interval intersecting region R, i.e., $1.28 \le y \le 4.4$, a polynomial of degree 20 suffices. By contrast, Algorithm 680 uses a degree of approximation ranging between 20 and 64 over the same interval.

If these rational expansions were to be incorporated in a software package, one could consider tailoring the value of N to the input argument z as well as the required accuracy. One indication of how this might be achieved is the error estimate (31). However, using a different N for each z will be inefficient since each N requires a new set of expansion coefficients. (Recall, the a_n depend on N through the optimal dependence $L = 2^{-1/4}N^{1/2}$.) Thus one would probably subdivide the first quadrant into various regions, restricting the algorithm to use only a few selected values of N with precomputed coefficients a_n. We will not discuss such implementation details here.

We conclude from these comparisons that the rational expansions are not as efficient as Taylor expansions and continued fractions for $|z|$ small and $|z|$ large, respectively. They are competitive, however, for intermediate $|z|$. At any rate, we feel the principal advantage of our method is that a single expansion provides high accuracy for the entire first quadrant, in contrast to Taylor expansions and continued fractions that break down completely in certain regions. This makes the rational expansions especially attractive for vectorized implementations such as the Matlab program given in Table 1. Also considering the ease of coding, we believe we have introduced here a method that may be effectively incorporated in both professional and personal software libraries.

Acknowledgments. The author is indebted to Walter Gautschi for pointing the way to Algorithms 363 and 680, to Enrique Thomann for helpful discussions, and especially to Nick Trefethen for taking a keen interest in this work. The major part of this research was performed during May–August 1992 at the Department of Computer Science, Cornell University, whose outstanding facilities and friendly people made it a pleasant experience. To all, my sincerest gratitude.

REFERENCES

[1] J. Boyd, *The optimization of convergence for Chebyshev polynomial methods in an unbounded domain*, J. Comput. Phys., 45 (1982), pp. 43–79.

[2] ———, *Chebyshev & Fourier Spectral Methods*, Springer-Verlag, Berlin, 1989.

[3] C. I. Christov, *A complete orthonormal system of functions in $L^2(-\infty, \infty)$ space*, SIAM J. Appl. Math., 42 (1982), pp. 1337–1344.

[4] W. J. Cody, *Rational Chebyshev approximations for the error function*, Math. Comp., 23 (1969), pp. 631–637.

[5] ———, *SPECFUN—A portable special function package*, in New Computing Environments: Microcomputers in Large-Scale Scientific Computing, A. Wouk, ed., Society for Industrial and Applied Mathematics, Philadelphia, PA, 1987, pp. 1–12.

[6] ———, *Performance evaluation of programs for the error and complementary error functions*, ACM Trans. Math. Software, 16 (1990), pp. 29–37.

[7] W. J. Cody, K. A. Paciorek, and H. C. Thacher, Jr., *Chebyshev approximations for Dawson's integral*, Math. Comp., 24 (1970), pp. 171–178.

[8] J. Dongarra and E. Grosse, *Distribution of mathematical software via electronic mail*, Comm. ACM, 30 (1987), pp. 403–407.

[9] A. Erdélyi, W. Magnus, F. Oberhettinger, and F. G. Tricomi, *Tables of Integral Transforms, Vol.* II, McGraw-Hill, New York, 1954.

[10] B. D. Fried and S. D. Conte, *The Plasma Dispersion Function, The Hilbert Transform of the Gaussian*, Academic Press, New York, 1961.

[11] V. N. Faddeeva and N. N. Terent'ev, *Tables of values of the function* $w(z) = e^{-z^2}(1 + (2i/\sqrt{\pi})\int_0^z e^{t^2}\,dt)$ *for complex argument*, Gosud. Izdat. Teh.-Teor. Lit., Moscow, 1954; English transl., Pergamon Press, New York, 1961.

[12] W. Gautschi, *Error function and Fresnel integrals*, in Handbook of Mathematical Functions, M. Abramowitz and I. A. Stegun, eds., Dover, New York, 1965, pp. 295–329.

[13] ———, *Algorithm 363—Complex error function*, Comm. ACM, 12 (1969), p. 635.

[14] ———, *Efficient computation of the complex error function*, SIAM J. Numer. Anal., 7 (1970), pp. 187–198.

[15] D. B. Hunter and T. Regan, *A note on the evaluation of the complementary error function*, Math. Comp., 26 (1972), pp. 539–541.

[16] P. Henrici, *Applied and Computational Complex Analysis, Vol.* 3, Wiley-Interscience, New York, 1986.

[17] *IMSL Library (Reference Manual), Vol.* 3, *Chap.* M, IMSL Inc., Houston, TX, 1982.

[18] N. L. Johnson and S. Kotz, *Continuous Univariate Distributions, Vol.* 2, Houghton-Mifflin, New York, 1970.

[19] C. Lanczos, *Applied Analysis*, Dover, New York, 1988.

[20] Y. Luke, *The Special Functions and their Approximations, Vol.* 2, Academic Press, New York, 1976.

[21] *Matlab Reference Guide*, The MathWorks Inc., Natick, MA, 1992.

[22] F. Matta and A. Reichel, *Uniform computation of the error function and other related functions*, Math. Comp., 25 (1971), pp. 339–344.

[23] M. Mori, *A method for the error function of real and complex variable with high relative accuracy*, Pub. Res. Inst. Math. Sci., Kyoto University, 19 (1983), pp. 1083–1094.

[24] *NAG Fortran Library Manual, Mark* 11, *Vol.* 6, Numerical Algorithms Group Ltd., Oxford, 1984.

[25] F. W. Olver, *Asymptotics and Special Functions*, Academic Press, New York, 1974.

[26] G. P. Poppe and C. M. Wijers, *More efficient computation of the complex error function*, ACM Trans. Math. Software, 16 (1990), pp. 38–46.

[27] ———, *Algorithm 680—Evaluation of the complex error function*, ACM Trans. Math. Software, 16 (1990), p. 47.

[28] J. B. Rosser, *Theory and Applications of* $\int_0^z e^{-x^2}\,dx$ *and* $\int_0^z e^{-p^2y^2}\,dy\int_0^y e^{-x^2}\,dx$, Mapleton House, Brooklyn, NY, 1948.

[29] J. L. Schonfelder, *Chebyshev expansions for the error and related functions*, Math. Comp., 32 (1978), pp. 1232–1240.

[30] I. A Stegun and R. Zucker, *Automatic computing methods for special functions. Part* IV. *Complex error function, Fresnel integrals, and other related functions*, J. Res. Nat. Bur. Standards, 86 (1981), pp. 661–670.

[31] J. A. Weideman, *The eigenvalues of Hermite and rational spectral differentiation matrices*, Numer. Math., 61 (1992), pp. 409–431.

[32] ———, *Computing the Hilbert transform on the real line*, Math. Comp., to appear.

[33] ———, *Computing integrals of the complex error function*, Proceedings of Symposia in Applied Mathematics: Mathematics of Computation 1943–1993, American Mathematical Society, Providence, RI, to appear.

[34] J. Wimp, *Computation with Recurrence Relations*, Pitman, Boston, 1984.

[35] R. Wong, *Asymptotic Approximation of Integrals*, Academic Press, Boston, 1989.